Biometals (2007) 20:807–820
DOI 10.1007/s10534-006-9044-9

Cadmium induces nuclear translocation of β-catenin and increases expression of *c-myc* and *Abcb1a* in kidney proximal tubule cells

Frank Thévenod · Natascha A. Wolff · Ulrich Bork · Wing-Kee Lee · Marouan Abouhamed

Received: 1 September 2006 / Accepted: 18 October 2006 / Published online: 29 November 2006

Abstract Cadmium (Cd^{2+}) induces renal proximal tubular (PT) damage, including disruption of the E-cadherin/β-catenin complex of adherens junctions (AJs) and apoptosis. Yet, chronic Cd^{2+} exposure causes malignant transformation of renal cells. Previously, we have demonstrated that Cd^{2+}-mediated up-regulation of the multidrug transporter Abcb1 causes apoptosis resistance in PT cells. We hypothesized that Cd^{2+} activates adaptive signaling mechanisms mediated by β-catenin to evade apoptosis and increase proliferation. Here we show that 50 μM Cd^{2+}, which induces cell death via apoptosis and necrosis, also causes a decrease of the transepithelial resistance of confluent WKPT-0293 Cl.2 cells, a rat renal PT cell model, within 45 min of Cd^{2+} exposure, as measured by electric cell-substrate impedance sensing. Immunofluorescence microscopy demonstrates Cd^{2+}-induced decrease of E-cadherin at AJs and redistribution of β-catenin from the E-cadherin/β-catenin complex of AJs to cytosol and nuclei after 3 h. Immunoblotting confirms Cd^{2+}-induced decrease of E-cadherin expression and translocation of β-catenin to cytosol and nuclei of PT cells. RT-PCR shows Cd^{2+}-induced increase of expression of *c-myc* and of the isoform *Abcb1a* at 3 h. The data prove for the first time that Cd^{2+} induces nuclear translocation of β-catenin in PT cells. We speculate that Cd^{2+} activates β-catenin/T-cell factor signaling to trans-activate proliferation and apoptosis resistance genes and promote carcinogenesis of PT cells.

Keywords Nephrotoxicity · Apoptosis · Multidrug resistance P-glycoprotein · Malignancy · T-cell factor/lymphoid enhancer factor

F. Thévenod (✉) · N. A. Wolff · U. Bork · W.-K. Lee · M. Abouhamed
Department of Physiology & Pathophysiology, University of Witten/Herdecke, Stockumer Str. 12, D-58448 Witten, Germany
e-mail: frank.thevenod@uni-wh.de

Introduction

Cadmium (Cd^{2+}) is a non-essential metal, which causes increasing concern as an environmental toxicant that also enters the food chain (Friberg et al. 1986; Singh and McLaughlin 1999). Following pulmonary or gastrointestinal absorption, Cd^{2+} is taken up by the liver where it forms complexes with small peptides and proteins via sulfhydryl groups, including glutathione (GSH) or the high affinity metal binding protein metallothionein (MT) (Coyle et al. 2002). Cd^{2+} is then either secreted into the bile or released into the circulation as CdGSH or CdMT complexes (Dudley et al. 1985).

Any bound or unbound Cd^{2+} that is released into the circulation and ultrafiltered by the

kidney glomeruli is reabsorbed by the S1-segment of the PT, because it possesses transport pathways and receptors for free Cd^{2+} as well as for the various forms of complexed Cd^{2+} (Thévenod 2003; Bridges and Zalups 2005; Wolff et al. 2006). Consequently, the S1-segment of the PT represents the primary target of Cd^{2+}-induced nephrotoxicity (Friberg et al. 1986; Thévenod 2003; Bridges and Zalups 2005), which can result in a general transport defect of the PT with proteinuria, aminoaciduria, glucosuria and phosphaturia.

The cellular processes underlying cadmium nephrotoxicity usually culminate in the triggering of cell death either by apoptosis or necrosis (for review, see (Zalups and Koropatnick 2000; Thévenod 2003)). PT apoptosis has been described in vivo (Liu et al. 1998; Takebayashi et al. 2000) and in vitro (Thévenod and Friedmann 1999). It can occur as early as 3 h after exposure to Cd^{2+} (Thévenod et al. 2000) and involves activation of the mitochondria-dependent pathway (Thévenod 2003; Lee et al. 2005). This entails the release of death promoting factors, such as cyt. *c* and apoptosis inducing factor (AIF) (Lee et al. 2005) and activation of calpain- and caspase-dependent apoptotic pathways (Lee et al. 2006).

Interestingly, exposure of kidney PT cells to low micromolar concentrations of Cd^{2+} may also induce the expression of cell survival genes, such as the proto-oncogenes *c-fos*, *c-jun*, and *c-myc* (Matsuoka and Call 1995), which promote cell proliferation. Genes coding for the synthesis of protective and/or anti-apoptotic molecules are also activated, including metallothioneins, glutathione, stress (heat shock) proteins, and the multidrug transporter Abcb1 (for review, see (Waisberg et al. 2003)). Previously, we have demonstrated that during exposure to 10 μM Cd^{2+} for up to 72 h apoptosis peaks at 24 h, but then decreases over time (Thévenod et al. 2000; Erfurt et al. 2003). This is caused by over-expression of Abcb1 that apparently contributes to apoptosis resistance in PT cells (Thévenod 2003). These protective and anti-apoptotic mechanisms induced by Cd^{2+} may be of utmost medical importance because chronic Cd^{2+} exposure has been found associated with cancers of the lung, prostate, pancreas and kidney and has therefore been classified as a class 1 carcinogen (IARC 1993). Further evidence has been provided by recent controlled epidemiological case studies, which have demonstrated an association between occupational Cd^{2+} exposure and renal cancer (Pesch et al. 2000; Hu et al. 2002).

One early event associated with Cd^{2+} nephrotoxicity is the alteration of the properties of adherens junctions (AJs) and tight junctions (TJs) due to Ca^{2+} displacement, which triggers disruption of the homophilic E-cadherin interaction. This causes a loss of the integrity of the cell–cell adhesion belt and disassembly of TJs (Rothen-Rutishauser et al. 2002), with a concomitant decrease in the transepithelial resistance and increased paracellular permeability. Cd^{2+} increased the paracellular permeability of the PT in vivo, which was associated with a redistribution of the TJ protein claudin-2 (Jacquillet et al. 2006). In vitro studies (Prozialeck and Niewenhuis 1991b; Zimmerhackl et al. 1998; Gennari et al. 2003) showed an increase in the paracellular permeability to small solutes and a decrease in transepithelial resistance induced by Cd^{2+}. This was associated with a decrease of E-cadherin expression in AJs of a PT cell line (Prozialeck and Niewenhuis 1991a) and PT of Cd^{2+}-treated rats (Prozialeck et al. 2003).

In addition to its structural role in AJs, β-catenin also functions as a latent signaling molecule that can act as a transcription factor in the nucleus by serving as a co-activator of the lymphoid enhancer factor (LEF)/T-cell factor (TCF) DNA-binding protein family (Conacci-Sorrell et al. 2002). As such, it trans-activates target genes that stimulate cell proliferation, e.g. *c-myc* and *cyclin D1*, but also genes that protect cells from apoptosis, such as *Abcb1* (for review, see (Conacci-Sorrell et al. 2002)).

Thus, the present study was designed to determine whether disruption of the E-cadherin/β-catenin complex, as observed during Cd^{2+} exposure, results in the release of β-catenin from the E-cadherin/β-catenin complex in the AJ pool and its translocation and accumulation in the nucleus to trans-activate target genes of the β-catenin/TCF complex, such as *c-myc* and *Abcb1a*.

Methods

Materials

ECIS 8W10E cell culture plates and μ-Slide 8-well plates were purchased from Integrated BioDiagnostics (Munich, Germany). The mouse monoclonal Clone 14 anti-β-catenin IgG1 antibody and the mouse monoclonal Clone 36 anti-E-Cadherin IgG2a antibody were obtained from BD Transduction Laboratories, (Heidelberg, Germany). Cy^{TM}3-conjugated donkey anti-mouse IgG (red) was from Jackson ImmunoResearch Laboratories Inc. (Cambridgeshire, UK). The horseradish peroxidase (HRP)-conjugated sheep anti-mouse immunoglobulin was obtained from GE Healthcare UK Limited (Little Chalfont, England). 3-(4,5-dimethyl-2-thiazolyl)-2,5-diphenyl-2H-tetrazolium bromide (MTT) was from Sigma (St. Louis, MO).

Methods

Cell culture

An immortalized cell line from the S1-segment of rat PT (WKPT-0293 Cl.2) (Woost et al. 1996) was cultured as previously described (Wolff et al. 2006). Cells were passaged (passage number <50) twice a week upon reaching confluency.

Isolation of cytoplasmic and nuclear protein extracts from WKPT-0293 Cl.2 cells

The protocol was adapted from the method described by Andrews and Faller (1991). Essentially, 5×10^5 cells per well were grown in standard culture medium for 48 h in 35 mm 6-well plates (Nunc, Wiesbaden, Germany). The medium was replaced by serum-free medium (SFM) and cells were incubated with or without 50 µM Cd^{2+} for 3 h. Cells were harvested into 400µl of ice cold buffer A (10 mM HEPES-KOH, pH 7.9, 1.5 mM $MgCl_2$, 10 mM KCl, 0.5 mM DTT, 0.2 mM Pefabloc SC), and allowed to swell and lyse on ice for 10 min. An aliquot of the cell suspension representing homogenate was collected for immunoblotting, and the remainder was centrifuged at 4°C and 15,800 × g for 10 s. The supernatant containing cytosolic proteins was removed and retained for immunoblotting. Exactly 100 µl of buffer B (20 mM HEPES-KOH, pH 7.9, 25% glycerol, 420 mM NaCl, 1.5 mM $MgCl_2$, 0.2 mM EDTA, 0.5 mM DTT, 0.2 mM Pefabloc SC) was added to the pellet and incubated on ice for 20 min. The suspension was centrifuged at 15,800 × g for 2 min and the supernatant containing the nuclear proteins was collected and aliquoted for immunoblotting.

Immunoblotting

Protein concentration of samples was determined by the Bradford method (Bradford 1976), using bovine serum albumin as a standard.

Exactly 20 µg protein of cell homogenates, cytosolic and nuclear proteins of cells ±50 µM Cd^{2+} in SFM for 3 h were mixed with 3-× Laemmli buffer, incubated for 5 min at 95°C and sonicated on ice. The 7.5% SDS-PAGE, transfer, antibody incubation and immunoblot development and visualization were performed as previously described (Abouhamed et al. 2006). Dilutions of primary anti-mouse β-catenin antibody and primary anti-human E-cadherin antibody were 1:500 and 1:2,000, respectively. HRP-conjugated secondary anti-mouse IgG antibody was diluted 1:10,000. Blots were scanned digitally and signals were evaluated by densitometry using TINA software (Raytest IsotopenmessgeräteGmbH, Straubenhardt, Germany), compatible with the TINA-PCBAS and TIFF files.

Immunofluorescence staining of WKPT-0293 Cl.2 cells

Exactly 9×10^4 cells were grown for 48 h on round glass coverslips with a diameter of 12 mm. The standard medium was then replaced by SFM medium and cells were incubated with or without 50 µM Cd^{2+} for 3 h. Immunofluorescence staining was performed as previously described (Abouhamed et al. 2006; Wolff et al. 2006). Anti-mouse β-catenin antibody was diluted 1:2000 and anti-human E-cadherin antibody was diluted 1:900. Cy^{TM}3-conjugated donkey anti-mouse IgG was diluted 1:600. Cells were counter-stained with 2′-(4-Ethoxyphenyl)-5-(4-methyl-1-piperazinyl)-

2,5′-bi-1H -benzimidazole · 3HCl (H-33342, 1 μg/ml), viewed using filters for Cy™3 and DAPI and acquired, processed and analyzed as described earlier (Abouhamed et al. 2006; Wolff et al. 2006).

Reverse transcriptase-polymerase chain reaction (RT-PCR)

WKPT-0293 Cl.2 cells were treated for 3 h ±50 μM Cd^{2+} in SFM in paired experiments. Total RNA was extracted from 1×10^7 cells using the RNeasy Mini Kit (Qiagen GmbH, Hilden, Germany) with on-column DNase digestion. First strand cDNA was synthesized with the Omniscript RT kit (Qiagen), using 1.0 μg of RNA per 20 μl reaction and oligo(dT) primer.

Abcb1a/1b (*mdr1a/1b*) and *c-myc* were amplified from WKPT-0293 Cl.2 cDNA by PCR with *GAPDH* as the standard, using the HotStarTaq Master Mix kit (Qiagen) with 4 vol% of RT reaction. After the initial activation step at 95°C for 15 min, PCR for *c-myc* and *GAPDH* were performed for 28 cycles of the following amplification parameters: 94°C for 20 s, 61.9°C for 30 s, 72°C for 45 s. Cycling conditions for *Abcb1a/1b* after the activation step were 35 cycles of 94°C for 20 s, 55°C for 20 s, 72°C for 30 s. The following primers (Operon Biotechnologies, Huntsville, AL) were used:

Rat *Abcb1a* forward 5′-GGACAGAAACAGAGGATCGC-3′
reverse 5′-CCCGTCTTGATCATGTGGCC-3′

Rat *Abcb1b* forward 5′-GGACAGAAACAGAGGATCGC-3′
reverse 5′-TCAGAGGCACCAGTGTCACT-3′

Rat *c-myc* forward 5′-AGCGTCCGAGTGCATCGACC-3′
reverse 5′-ACGTTCCAAGACGTTGTGTG-3′

Rat *GAPDH* forward 5′-AATGCATCCTGCACCACCAACTGC-3′
reverse 5′-GCGGCATGTCAG-ATCCACAACGG-3′

Primers and cycling conditions for rat *Abcb1a/1b* were chosen according to Lee et al. (2001). Primers for *c-myc* were designed with the Fast-PCR program version 3.6 (University of Helsinki, Institute of Biotechnology), using the GenBank sequence of rat *c-myc* (Accession number Y00396). The upstream primer sequence for GAPDH was taken from Harrison-Bernard et al. (1999). Control reactions for each primer pair were also performed without RT, or with water instead of cDNA template. PCR products were separated on 1.5% agarose gels containing 0.01% GelRed (Biotium, Hayward, CA), loading 9 μl PCR reaction per lane.

Electric cell-substrate impedance sensing (ECIS)

The ECIS technology is based on non-invasive live measurements of frequency-dependent changes in total electrical impedance (Z) of cell-covered gold-film electrodes to alternating current (AC using an ECIS™1600R instrument (Applied BioPhysics). The current flows between 250 μm-diameter electrodes (1–10 depending on the array type) and a larger counter-electrode, which are attached to the bottom of ECIS cell culture wells, using culture medium as the electrolyte. Without cells, the current flows unrestrained from the surface of the electrodes. When cells attach and spread on the surface of planar gold-film electrodes they behave like insulating particles that hinder current flow from the electrode into the bulk electrolyte and thereby increase the overall electrode impedance. Z is given by the AC equivalent of Ohm's law: $Z = V/I$. The ECIS™1600R instrument breaks down the impedance into two parts—one due to resistance (R) and the other to the reactance (X_c) of the system, which is due to the capacitance (C) associated with the gold surfaces in the tissue culture medium. Hence, the total impedance is given by $Z = (R^2 + X_c^2)^{0.5}$. The basic principles of the method are described elsewhere (Giaever and Keese 1991; Wegener et al. 2000).

Practically, Z values of cell-free electrodes and electrodes covered with a confluent monolayer of WKPT-0293 Cl.2 cells are sampled at different frequencies. The difference in R of cell-free

electrodes as opposed to the same electrodes covered with a cell monolayer passes a maximum at 400 Hz, whereas the difference in C of electrodes without and with cells reaches a maximum at 40 kHz, indicating that impedance readings at these two frequencies are most sensitive to mirror the associated respective changes in electrode R and C (Giaever and Keese 1991). A change of R at 400 Hz mainly reflects alterations of the paracellular electrical properties of the monolayer (i.e. changes of the permeability of tight-junctions), provided C remains constant (Giaever and Keese 1991; Wegener et al. 2000). An additional increase of C at 40 kHz mirrors a loss of monolayer integrity.

Exactly 1.5×10^5 WKPT-0293 Cl.2 cells/well (passage numbers <50) were plated on ECIS 8W10E cell culture plates at 37°C and incubated with 5% CO_2. For Cd^{2+} experiments, the culture medium of functional monolayers was changed to SFM. No changes in C or R were observed after changing from standard serum containing medium to SFM in control cells. Z of the 10 gold electrodes in each well was measured every 9 min at different frequencies. C and R values were calculated from the Z values and the corresponding changes in phases of AC by the ECIS software.

For phase contrast microscopy of control and Cd^{2+}-treated WKPT-0293 Cl.2 cells, experiments were performed simultaneously with the ECIS measurements, using μ-Slide 8-well plates. Images were captured, acquired, processed and analyzed as described for immunofluorescence microscopy.

MTT cell toxicity assay

Exactly 5×10^3 cells were grown for 48 h in serum containing medium until they reached a confluency of about 30%. The standard medium was then replaced by SFM medium and cells were incubated in the absence or presence of 50 μM Cd^{2+} for 3 h. The MTT assay is a measurement of cell viability, hence it does not distinguish between apoptosis, necrosis or inhibition of cell growth (Mosmann 1983). MTT, a yellow tetrazolium salt is metabolyzed by active succinate dehydrogenase in the mitochondria of living cells into a blue formazan product. Hence, the MTT method is a measure of mitochondrial function. Assays were conducted according to Denizot and Lang (Denizot and Lang 1986), as previously described (Lee et al. 2006). Reference wavelength values were subtracted from test wavelength values and the differences obtained in controls were set to 100%, which was equivalent to 0% cell death.

Statistical analyses

Representative data or means ± S.E.M. are shown. Statistical analysis using unpaired Student's t-test was carried out with Sigma Plot 8.0 (Inc., Chicago, IL). For more than two groups, one-way ANOVA was used assuming equality of variance with Levene's test and Tukey post hoc test for pairwise comparison with SPSS 12.0. Results with $P \leq 0.05$ were considered to be statistically significant. To obtain EC_{50} values, individual dose-response curves of Cd^{2+} cytotoxicity were fitted using the Sigma Plot 8.0 spreadsheet program assuming a sigmoidal dose response.

Results

Assessment of E-cadherin and β -catenin expression in WKPT-0293 Cl.2 cells by immunofluorescence labelling and immunoblotting

Cell–cell contacts are formed at the adherens junctions (AJs) by intercellular Ca^{2+}-dependent E-cadherin homodimer formation (Vleminckx and Kemler 1999; Miyoshi and Takai 2005). To assay for the explression of E-cadherin by rat PT cells, immunofluorescence distribution of the protein was investigated on confluent monolayers of WKPT-0293 Cl.2 cells. Monolayers demonstrated the typical pattern of E-cadherin expression at the cell borders (Fig. 1A). Expression of the E-cadherin protein in WKPT-0293 Cl.2 cells was further confirmed by immunoblotting, where

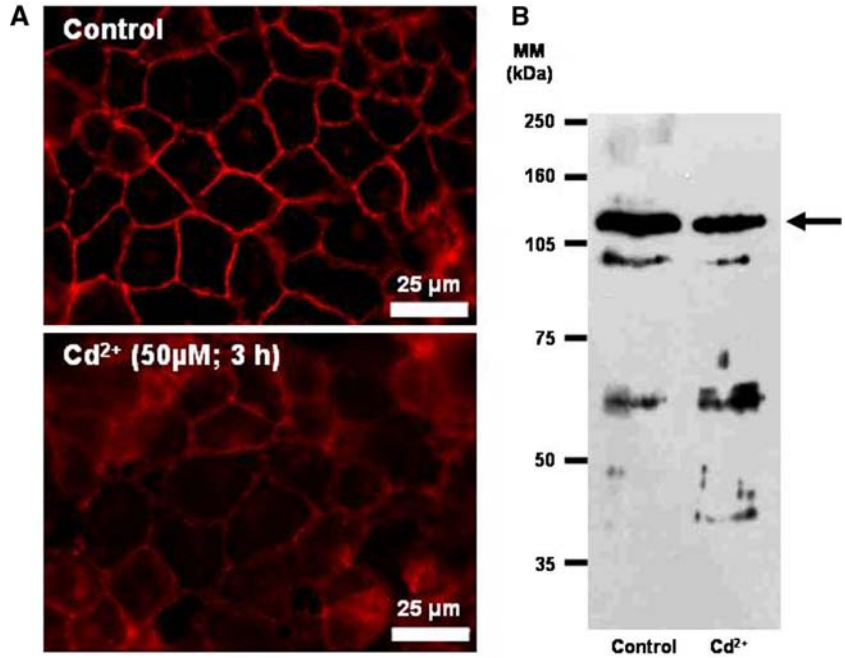

Fig. 1 Expression and cellular localization of E-cadherin in WKPT-0293 Cl.2 cells. (**A**) Immunofluorescence labelling of E-cadherin in PT cells. Cells were treated ±50 µM Cd^{2+} for 3 h prior to immunostaining using an E-cadherin primary antibody (1:900) and secondary $Cy^{TM}3$-conjugated antibody (1:600). (**B**) E-cadherin immunoreactivity in WKPT-0293 Cl.2 cells. Cell homogenates (50 µg protein) from PT cells ±50 µM Cd^{2+} for 3 h were separated by SDS-PAGE on 7.5% acrylamide gels. Blots were incubated with anti-human E-cadherin antiserum (1:2,000). Sizes (in kDa) of molecular mass (MM) markers are indicated on the left. The arrow indicates E-cadherin with an approximate MM of 120 kDa

the E-cadherin antibody recognized a protein of ~120 kDa, which is the predicted molecular mass of E-cadherin (Fig. 1B).

β-catenin normally associates with E-cadherin and with α-catenin and thereby participates in the regulation of cell-to-cell adhesion (Vleminckx and Kemler 1999; Miyoshi and Takai 2005). WKPT-0293 Cl. 2 cells also express β-catenin. As shown in Fig. 2A, fluorescence labeling was mainly distributed along the cell borders, but was also weakly expressed in the cytosol, indicating that even under control conditions β-catenin is not exclusively bound to E-cadherin (Gottardi et al. 2001). This distribution was confirmed by immunoblotting, where the antibody recognized a major immunoreactive band in PT cell homogenate at the predicted molecular mass of 92 kDa (first lane of Fig. 3A). Figure 3A also shows that in control cells some cellular β-catenin was distributed to the cytosolic and nuclear fractions of PT cells.

Capacitance and resistance changes measured with the ECIS technique and changes in cellular morphology and cell viability of WKPT-0293 Cl.2 cells induced by Cd^{2+}

When cells were plated at a density of 1.5×10^5 cells/well in serum containing medium the resistance (R) increased slowly from values of the cell-free electrode to its final values after 40–55 h (data not shown), reflecting the establishment of a monolayer with functional tight-junctions that restricts the current flow between neighboring cells (Wegener et al. 2000). Simultaneous measurements of the electrode capacitance (C) reflected cell attachment, spreading and proliferation. The cell-free area of the electrode decreased and C dropped to reach a baseline of ~8 nF after 40–55 h, when an intact monolayer (shown in Fig. 4B, 0 h Cd^{2+}) was formed.

For Cd^{2+} experiments, the culture medium of functional monolayers was changed to SFM. No

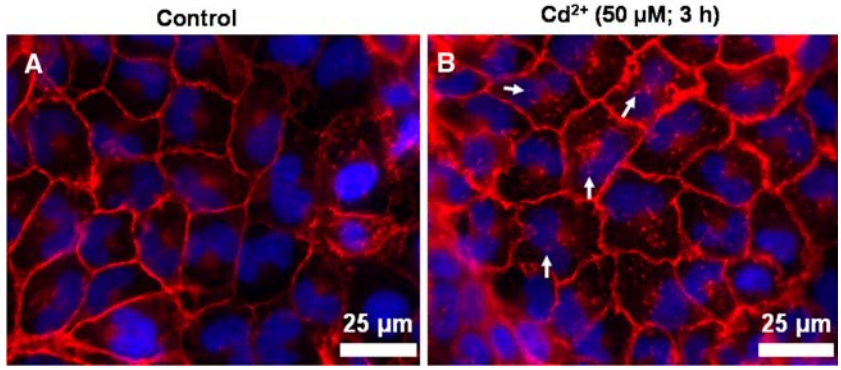

Fig. 2 Effect of Cd^{2+} on the intracellular distribution of β-catenin in WKPT-0293 Cl.2 cells. Cells were incubated without (**A**) or with 50 µM $Cd^{2+}$for 3 h (**B**) prior to immunostaining using a β-catenin primary antibody (1:2000) and secondary $Cy^{TM}3$-conjugated antibody (1:600). Nuclei were counter-stained with H-33342 (blue) (1 µg/ml). Arrows indicate nuclear β-catenin immunolabelling after Cd^{2+} exposure

changes in *C* or *R* were observed after changing from serum containing medium to SFM in control cells (not shown). Changes in *R* and *C* of WKPT-0293 Cl.2 cell monolayers during incubation with 50 µM Cd^{2+} over 4 h were then monitored. Within 45 min after addition of 50 µM Cd^{2+} to the medium, *R* began to steadily decrease, whereas the corresponding *C* values still remained stable at the baseline (Fig. 4A). In simultaneously performed control experiments without Cd^{2+}, both parameters were unchanged throughout the experimental period of 4 h (Fig. 4A). After 90 min Cd^{2+} exposure, *R* values had dropped to about 60% of the control values. At this time *C* started to increase, indicating that the integrity of the cell monolayer began to disrupt. Still, no major change in the morphology of the epithelial monolayer could be observed (Fig. 4B, 1.5 h Cd^{2+}). However, after 3 h, a number of cells were rounded or detached (arrows in Fig. 4B, 3 h Cd^{2+}), which was paralleled by a substantial increase of *C* by about 2.5-fold (Fig. 4A). Hence, the ECIS measurements of confluent WKPT-0293 Cl.2 cells indicate that 50 µM Cd^{2+} affects the paracellular permeability within 45 min, possibly by displacement of Ca^{2+} from and/or interaction of Cd^{2+} with E-cadherin homodimers (Prozialeck et al. 2002), resulting in disassembly of adherens and tight-junctions (Rothen-Rutishauser et al. 2002). At later time points, cell damage most likely induced by Cd^{2+} uptake and cellular toxicity resulted in an

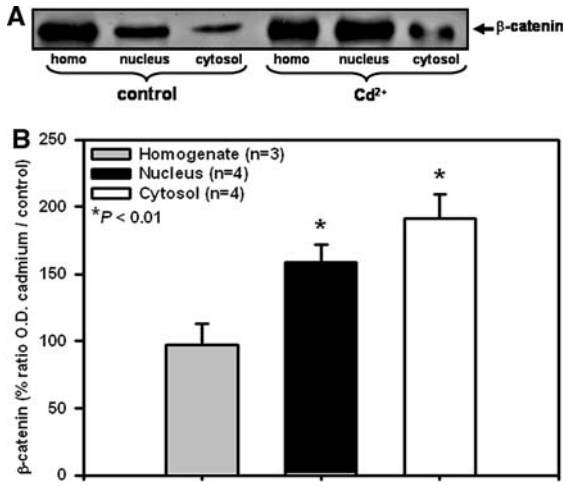

Fig. 3 Cd^{2+} induces translocation of β-catenin to cytosol and nuclei of WKPT-0293 Cl.2 cells. (**A**) β-catenin protein immunoreactivity in PT cells. Cytosolic (cytosol) and nuclear (nucleus) proteins from controls and Cd^{2+}-treated (50 µM; 3 h) PT cells were fractionated from cell homogenate (homo) as described in ''Methods''. Equal amounts of protein (20 µg) were loaded onto 7.5% acrylamide gels. Blots were incubated with β-catenin antiserum (1:500). (**B**) Semiquantitative analysis of β-catenin protein immunoreactivity in PT cells ±Cd^{2+} exposure (50 µM; 3 h). Immunoblotting signals were evaluated by densitometry. The ratio of the optical density (O.D.) of signals from Cd^{2+} treated cells over controls was calculated and expressed as % of controls. *Indicates a significant difference ($P < 0.01$) in Cd^{2+}-treated cells compared to controls using unpaired Student's *t*-test

increase of *C* reflecting changes in cell shape, decreased adherence and loss of integrity of the epithelial monolayer (Wegener et al. 2000; Arndt

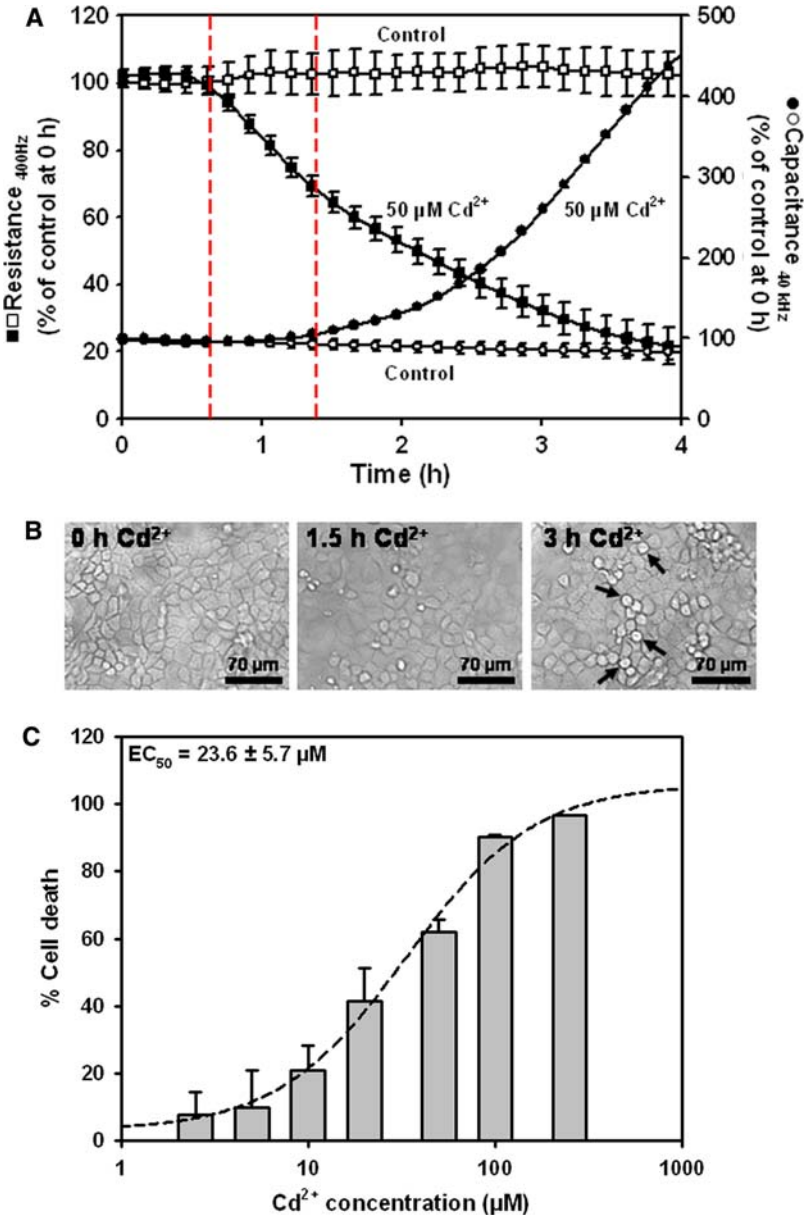

Fig. 4 Effect of Cd^{2+} on the electrical properties and cell viability of confluent WKPT-0293 Cl.2 cell monolayers. (**A**) At time 0, confluent monolayers of PT cells grown in 8-well ECIS arrays were treated with 50 µM Cd^{2+} (filled symbols) or left untreated (open symbols). Electrode resistance (R) measured at 400 Hz (squares) and electrode capacitance (C) measured at 40 kHz (circles) were simultaneously recorded. The area between the dashed vertical lines indicates the time window for a decrease of transepithelial resistance without a decrease of monolayer integrity (see ''Methods''). Values are given as a percentage of control R (4.5 kΩ ±0.1; n = 3) and C (7.8 nF ± 0.9; n = 3). Means ± SEM of 3 – 6 separate experiments are shown. (**B**) Phase contrast microscopy of control and Cd^{2+}-treated PT cells. In parallel experiments, PT cells were grown on μ-Slide 8 well plates for phase contrast microscopy. Monolayer integrity was determined qualitatively by estimating rounded or detached cells (arrows) after 0, 1.5 and 3 h of exposure to 50 µM Cd^{2+}. (**C**) Cell viability of PT cells as a function of the Cd^{2+} concentration. Cells (5×10^3 per well) were grown for 48 h prior to incubation with different Cd^{2+} concentrations in SFM for 3 h. Cell viability was determined using the MTT assay. Means ± SEM of 2–9 separate experiments are shown, where applicable. EC_{50} was derived using a curve fitting that assumed a sigmoidal dose-response. The mean EC_{50} value ± SEM of 9 different individual experiments is also indicated

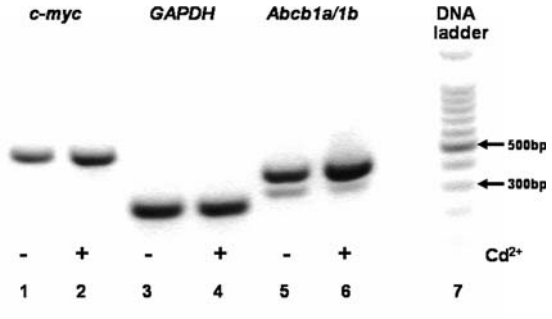

Fig. 5 Upregulation of *c-myc* and *Abcb1a* mRNA in WKPT-0293 Cl.2 cells upon Cd^{2+} exposure. First-strand cDNA was synthesized from RNA isolated from WKPT cells incubated for 3 h at 37°C in serum-free medium without (–) or with (+) 50 μM Cd^{2+}. PCR was then performed with primers specific for rat *c-myc* (538 bp), rat *Abcb1a* (441 bp) and *Abcb1b* (356 bp), or rat *GAPDH* (300 bp) as a house-keeping gene. Equal volumes of products were run on a 1.5% agarose gel stained with GelRed. This result was reproducible in 4 out of 4 different experiments for *c-myc* and in 5 out of 7 experiments for *Abcb1a/1b*

et al. 2004). Cell viability experiments following exposure to different concentrations of Cd^{2+} for 3 h, which were determined with the MTT assay, indicated a concentration-dependent increase of cytotoxicity and death with an EC_{50} of ~25 μM and about 60% cytotoxicity at 50 μM Cd^{2+} (Fig. 4C).

Cd^{2+} decreases E-cadherin expression and increases cytosolic and nuclear distribution of β -catenin in WKPT-0293 Cl.2 cells

As shown in Fig. 1A, in cells incubated with 50 μM Cd^{2+} for 3 h in SFM, E-cadherin expression at the cell borders was diminished, probably as a consequence of disruption of the homodimeric E-cadherin interaction and subsequent degradation (Vleminckx and Kemler 1999; Rothen-Rutishauser et al. 2002; Miyoshi and Takai 2005). Accordingly, immunoblotting showed a decrease of E-cadherin protein expression in homogenate from WKPT-0293 Cl.2 cells and an increase of a degradation product with a molecular mass of about 60 kDa (Fig. 1B). Figure 2B demonstrates that in cells treated with 50 μM Cd^{2+} for 3 h in SFM, β-catenin expression at the cell borders was fuzzy and irregular, suggesting disassembly of the E-cadherin/β-catenin complex. Dotty β-catenin labelling was detected in the cytosol and at perinuclear sites of most cells, but also in the nucleus of certain cells (arrows in Fig. 2B). A similar redistribution was already observed after 1–2 h of exposure of PT cells to 50 μM Cd^{2+}, but was less obvious (data not shown). Moreover, when cells were pre-treated with the proteasomal inhibitors MG132 or lactacystin (10 μM with 2 h pre-incubation; 50 μM Cd^{2+} for 1–3 h) (Thévenod and Friedmann 1999), cytosolic and nuclear β-catenin labelling was enhanced (data not shown) suggesting that β-catenin released from the AJs is partially degraded by the proteasome. To verify the immunofluorescence microscopy data, nucleic and cytosolic proteins of controls and of cells treated with 50 μM Cd^{2+} for 3 h were fractionated and immunoblotting of β-catenin was performed. A representative immunoblot shows an increase of β-catenin in both nucleus and cytosol of Cd^{2+}-treated cells compared to controls (Fig. 3A). To quantify the changes in cellular distribution of β-catenin after Cd^{2+} treatment, the ratio of the optical density of immunoreactive signals in Cd^{2+}-treated and control cells was calculated. As shown in Fig. 3B, a significant increase of nuclear and cytosolic β-catenin induced by exposure to 50 μM Cd^{2+} for 3 h by 64.0 ± 7.9% and 91.5 ± 17.5%, ($n = 4$; $P < 0.01$), respectively, was observed, whereas total β-catenin in the cell homogenate was not affected by Cd^{2+} treatment, indicating redistribution rather than an increased expression of β-catenin. Taken together, the immunofluorescence and immunoblotting data demonstrate for the first time that 50 μM Cd^{2+} for 3 h causes disruption of E-cadherin/β-catenin complexes of AJs and degradation of E-cadherin, but also induces a redistribution of β-catenin from the E-cadherin/β-catenin complexes at the AJs of the plasma membrane to cytosol and nuclei of WKPT-0293 Cl.2 cells.

Cd^{2+} increases mRNA expression of target genes of the β -catenin-T-cell factor transcription factor complex in WKPT-0293 Cl.2 cells

In addition to its structural role in AJs, β-catenin may function as a latent signaling molecule that can act as a transcription factor in the nucleus by serving as a co-activator of the lymphoid enhancer factor (LEF)/T-cell factor (TCF) family of DNA-binding proteins, which trans-activate genes that stimulate cell proliferation, such as *cyclin D1* and *c-myc*, but also genes that protect cells from apoptosis, such as *Abcb1* (for review, see (Conacci-Sorrell et al. 2002)). Hence, we investigated whether Cd^{2+} exposure activates target genes of the β-catenin/(LEF)/TCF transcriptional activator complex in WKPT-0293 Cl.2 cells. mRNA expression of *c-myc* and *Abcb1a/1b* was compared to that of the housekeeping gene *GAPDH* by RT-PCR in control cells and cells that had been exposed to 50μM Cd^{2+} for 3 h, which is the time frame of nuclear translocation of β-catenin (Figs. 2 and 3). As shown in the representative experiment of Fig. 5, *c-myc* was up-regulated by 3 h of exposure to 50 μM Cd^{2+} (Fig. 5, compare lane 2 to the control in lane 1), whereas *GAPDH* was not affected by Cd^{2+} treatment (Fig. 5, lanes 3 and 4). *Abcb1a* and *Abcb1b* have similar expression levels in the kidney, where they are mainly located in the apical membrane of proximal tubule cells (Schinkel et al. 1994). In WKPT-0293 Cl.2 cells, *Abcb1a* appeared to have a higher expression level than *Abcb1b* (Fig. 5, lane 5). Exposure of cells to 50 μM Cd^{2+} for 3 h increased *Abcb1a* expression, but not *Abcb1b* (Fig. 5, compare the control in lane 5 to Cd^{2+} in lane 6). These data suggest that Cd^{2+}-induced translocation of β-catenin to the nucleus induces a trans-activation of specific target genes of the β-catenin/TCF complex, including *c-myc* and *Abcb1a*.

Discussion

The aim of the present study was to investigate whether Cd^{2+} exposure, apart from its known apoptosis-inducing effects, causes E-cadherin/β-catenin disruption to trigger a signaling pathway that may contribute to apoptosis resistance and cancer development. First, we demonstrated by immunoblotting and immunolocalization that the rat PT cell line WKPT-0293 Cl.2 expresses both components of the AJ complex of E-cadherin (Fig. 1) and β-catenin (Figs. 2A and 3A). Next we investigated the effect of Cd^{2+} on transepithelial resistance of confluent PT cells. Exposure of PT cells to 50 μM Cd^{2+} resulted in a rapid decrease of transepithelial resistance occurring within 45 min, as measured with the ECIS technique (Fig. 4A). These effects occurred prior to manifest cellular damage and death (Fig. 4), which confirms previous studies in LLC-PK1 cells (Niewenhuis et al. 1997). The changes of transepithelial resistance suggested a disassembly of the E-cadherin/β-catenin complex and subsequent disruption of TJs (Rothen-Rutishauser et al. 2002; Miyoshi and Takai 2005). In fact, Cd^{2+} exposure was associated with disruption of the E-cadherin/β-catenin complex and degradation of E-cadherin, which was reflected by a decrease of E-cadherin expression at the cell borders (Fig. 1A) and a concomitant reduction of total cellular E-cadherin protein content (Fig. 1B), a diffuse membrane staining for β-catenin (Fig. 2B) and an increase of β-catenin in the cytosol (Fig. 3B).

Cd^{2+}-induced interference with the E-cadherin/β-catenin complex, AJ disruption and a decrease of the transepithelial resistance have been previously demonstrated in vitro (Prozialeck and Niewenhuis 1991b; Prozialeck and Niewenhuis 1991a; Zimmerhackl et al. 1998; Gennari et al. 2003) and in vivo (Prozialeck et al. 2003) and were confirmed in the present study with our cell line (Fig. 4). E-cadherins are indirectly linked to the cortical actin cytoskeleton through β-catenin and α-catenin (Vleminckx and Kemler 1999; Miyoshi and Takai 2005). Consequently, Cd^{2+}-induced disruption of the E-cadherin/β-catenin complex may lead to a reorganization of the actin cytoskeleton, which has been demonstrated in rat kidney PT (Sabolic et al. 2001) and in PT cell lines (Prozialeck and Niewenhuis 1991b; Zimmerhackl et al. 1998).

Our data demonstrate for the first time that Cd^{2+} induces a subsequent translocation of

β-catenin to the nucleus, which was suggested by the localization of β-catenin immunofluorescence in the cytosol and the nucleus after Cd^{2+} exposure for 3 h (Fig. 2B, arrows) and proven by demonstrating an increase in the proportion of cytosolic and nuclear β-catenin in Cd^{2+}-treated cells compared to controls (Fig. 3B).

Cd^{2+}-induced disruption of the E-cadherin/β-catenin complex and the decrease of the transepithelial resistance have been previously found to be associated with reduced proliferation and cell death of PT cells (Zimmerhackl et al. 1998). We detected rounding up of PT cells after 3 h of exposure to 50 μM Cd^{2+} (Fig. 4B, arrows) and about 60% cytotoxicity, as determined with the MTT cell viability assay (Fig. 4C), which correlated with an increase of the electrode capacitance in the ECIS measurements (Fig. 4A). Though the Cd^{2+} concentration of 50 μM used in the present cellular study to induce a disruption of the E-cadherin/β-catenin complex and a decrease of transepithelial resistance may appear relatively high, the effective free Cd^{2+} concentration may actually be far lower, because Cd^{2+} will nonspecifically bind to many surface proteins. Humans and animals exposed to Cd^{2+} in real life may accumulate Cd^{2+} in kidney cells to concentrations far exceeding 50 μM. The threshold kidney Cd^{2+} concentration at which renal tubular dysfunction develops is estimated to be about 200 μg/g tissue (equivalent to 1–2 mM) for long term exposures (Friberg et al. 1986). This is in part due to the fact that intracellular Cd^{2+} induces the synthesis of metallothioneins, low-molecular-weight proteins that bind Cd^{2+} ions (Coyle et al. 2002) and thereby lower free Cd^{2+} concentration, which is toxic to the cells (Thévenod 2003).

The nephrotoxic effect of Cd^{2+} is well documented in vivo (Liu et al. 1998; Takebayashi et al. 2000) and in vitro (Thévenod and Friedmann 1999; Thévenod 2003; Lee et al. 2005): However, aside from its pro-apoptotic and necrotic potency, Cd^{2+} at the same time triggers a variety of cellular pathways and processes that aim at counter-acting toxicity and promoting cell survival and proliferation, and thereby may contribute to malignant transformation of mutated or pre-malignant cells. For example, chronic Cd^{2+} exposure of rat liver epithelial cells is associated with specific suppression of JNK1/2 signaling, which may result in apoptotic resistance and contribute to the development of malignancy (Qu et al. 2006). Moreover, induction of stress response genes by Cd^{2+}, such as heat shock protein 70, will limit cell damage (Gennari et al. 2003), whereas oxidative stress-mediated induction of the proto-oncogenes *c-jun*, *c-fos* and *c-myc* will promote cell proliferation (Matsuoka and Call 1995; Beyersmann and Hechtenberg 1997).

Because β-catenin is thought to represent a latent oncogen that forms a complex with the transcription factor TCF/LEF to trans-activate cell proliferation and survival genes (Polakis 1999), we hypothesized that Cd^{2+}-induced translocation of β-catenin to the nucleus might enhance transcription of these genes. Indeed, within 1.5–3 h of Cd^{2+} exposure, *c-myc* and *Abcb1* mRNAs were increased (Fig. 5), which confirms previous observations in other renal cell lines (Chin et al. 1990; Matsuoka and Call 1995). *Abcb1a* was the predominant isoform expressed in WKPT-0293 Cl.2 cells and was accordingly up-regulated by Cd^{2+}, whereas *Abcb1b* expression was not affected (Fig. 5). Prolonged exposure of PT cells to Cd^{2+} for up to 72 h has previously been found to result in increased resistance to apoptosis, which was in part due to up-regulation of the Abcb1 protein (Thévenod et al. 2000). We observed the effects of Cd^{2+} on the E-cadherin/β-catenin complex and transepithelial resistance (Figs. 1–4) at the same Cd^{2+} concentration that is known to induce apoptotic cell death in our cellular model (Lee et al. 2006), which confirms previous data obtained in LLC-PK1 cells (Zimmerhackl et al. 1998). Conversely, Cd^{2+} at low micromolar concentrations (5–20 μM) has been shown to induce both up-regulation of *Abcb1* and *c-myc* but also apoptosis in kidney cells (Chin et al. 1990; Matsuoka and Call 1995; Thévenod et al. 2000), indicating that damage to AJs, trans-activation of *Abcb1a* and *c-myc*, and induction of cell death may all be elicited at the same Cd^{2+} concentrations.

Activation of β-catenin/TCF signaling evokes increased trans-activation of the proliferation genes *c-myc* and *cyclin D1* as well as of the cell survival gene *Abcb1* (for review, see (Conacci-Sorrell et al. 2002)). Interestingly, trans-activa-

tion of *Abcb1* seems to be causative in the development of FAP (familial adenomatous polyposis)-syndrome, an inherited carcinoma of epithelial cells of the colon (Yamada et al. 2003).

Epithelial tissues form a protective barrier against the environment. They are characterized by a high rate of proliferation and are also constantly exposed to endogenous and exogenous toxicants, which render them particularly susceptible to mutations and development of malignancies. Due to its association with cancers of the lung, prostate, pancreas and kidney, Cd^{2+} has been classified as a class 1 carcinogen (IARC 1993). There is a general consensus that Cd^{2+} has no direct genotoxic effect (Verougstraete et al. 2002), however, chronic Cd^{2+} exposure may result in malignant transformation of cells that have been simultaneously exposed to other genotoxic compounds (Verougstraete et al. 2002). Cd^{2+} may contribute to carcinogenesis by indirect mechanisms, such as interference with DNA repair mechanisms (Jin et al. 2003), generation of reactive oxygen species, imbalance between pro- and anti-apoptotic mechanisms, etc. (reviewed in (Waisberg et al. 2003)). Apoptosis protects cells against oncogenesis through elimination of mutant or transformed cells. The development of tumor cell populations is determined by the rate of cell proliferation relative to the rate of apoptosis. Evasion of programmed cell death is a hallmark of cancer development (Hanahan and Weinberg 2000). Thus, the study of the mechanisms of acquired resistance to apoptosis in carcinogenesis could have important implications in both tumor initiation and progression of renal carcinomas.

In summary, we provide evidence indicating that micromolar Cd^{2+} concentrations decrease transepithelial resistance of confluent PT cells within 45 min of exposure. This is associated with disruption of the E-cadherin/β-catenin complex of AJs, degradation of E-cadherin and the release of β-catenin into the cytosol and nucleus. The increase of nuclear β-catenin correlates with an increased expression of the mRNA for *c-myc* and *Abcb1*, suggesting that the β-catenin/TCF transcription factor trans-activates both genes. Thus, Cd^{2+}-mediated activation of the β-catenin/TCF complex and trans-activation of genes for proliferation and cell survival may contribute to the development of resistance to apoptosis, ultimately leading to kidney cancer.

Acknowledgments We thank Dr. U. Hopfer (Case Western Reserve University, Cleveland, OH) for providing the cell line and Dr. Joachim Wegener (Institute for Biochemistry, University of Münster, Germany) for expert advice in setting up the ECIS technology and valuable discussions. This study was supported by the Deutsche Forschungsgemeinschaft (TH 345/8–1 and 8–2) and start-up funds from the University of Witten/Herdecke.

References

Abouhamed M, Gburek J, Liu W et al. (2006) Divalent metal transporter 1 in the kidney proximal tubule is expressed in late endosomes/lysosomal membranes: implications for renal handling of protein-metal complexes. Am J Physiol Renal Physiol 290:F1525-F1533

Andrews NC, Faller DV (1991) A rapid micropreparation technique for extraction of DNA-binding proteins from limiting numbers of mammalian cells. Nucleic Acids Res 19:2499

Arndt S, Seebach J, Psathaki K, Galla HJ, Wegener J (2004) Bioelectrical impedance assay to monitor changes in cell shape during apoptosis. Biosens Bioelectron 19:583–594

Beyersmann D, Hechtenberg S (1997) Cadmium, gene regulation, and cellular signalling in mammalian cells. Toxicol Appl Pharmacol 144: 247–261

Bradford MM (1976) A rapid and sensitive method for the quantitation of microgram quantities of protein utilizing the principle of protein-dye binding. Anal Biochem 72:248–254

Bridges CC, Zalups RK (2005) Molecular and ionic mimicry and the transport of toxic metals. Toxicol Appl Pharmacol 204:274–308

Chin KV, Tanaka S, Darlington G, Pastan I, Gottesman MM (1990) Heat shock and arsenite increase expression of the multidrug resistance (MDR1) gene in human renal carcinoma cells. J Biol Chem 265: 221–226

Conacci-Sorrell M, Zhurinsky J, Ben-Zeév A (2002) The cadherin-catenin adhesion system in signaling and cancer. J Clin Invest 109:987–991

Coyle P, Philcox JC, Carey LC, Rofe AM (2002) Metallothionein: the multipurpose protein. Cell Mol Life Sci 59:627–647

Denizot F, Lang R (1986) Rapid colorimetric assay for cell growth and survival. Modifications to the tetrazolium dye procedure giving improved sensitivity and reliability. J Immunol Methods 89:271–277

Dudley RE, Gammal LM, Klaassen CD (1985) Cadmium-induced hepatic and renal injury in chronically exposed rats: likely role of hepatic cadmium-metallothionein in nephrotoxicity. Toxicol Appl Pharmacol 77:414–426

Erfurt C, Roussa E, Thévenod F (2003) Apoptosis by Cd2+ or CdMT in proximal tubule cells: different

uptake routes and permissive role of endo/lysosomal CdMT uptake. Am J Physiol Cell Physiol 285: C1367-C1376

Friberg L, Elinder CG, Kjellstrom T, Nordberg GF (1986) Cadmium and health: a toxicological and epidemiological approach. CRC Press, Boca Raton FL

Gennari A, Cortese E, Boveri M, Casado J, Prieto P (2003) Sensitive endpoints for evaluating cadmium-induced acute toxicity in LLC-PK1 cells. Toxicology 183:211–220

Giaever I, Keese CR (1991) Micromotion of mammalian cells measured electrically. Proc Natl Acad Sci USA 88:7896–7900

Gottardi CJ, Wong E, Gumbiner BM (2001) E-cadherin suppresses cellular transformation by inhibiting beta-catenin signaling in an adhesion-independent manner. J Cell Biol 153:1049–1060

Hanahan D, Weinberg RA (2000) The hallmarks of cancer. Cell 100:57–70

Harrison-Bernard LM, El-Dahr SS, O'Leary DF, Navar LG (1999) Regulation of angiotensin II type 1 receptor mRNA and protein in angiotensin II-induced hypertension. Hypertension 33:340–346

Hu J, Mao Y, White K (2002) Renal cell carcinoma and occupational exposure to chemicals in Canada. Occup Med (Lond) 52:157–164

IARC (1993) Beryllium, cadmium, mercury, and exposures in the glass manufacturing industry. International agency for research on cancer monographs on the evaluation of carcinogenic risks to humans, vol. 58. IARC Scientific Publications, Lyon, pp 1–415

Jacquillet G, Barbier O, Cougnon M et al (2006) Zinc protects renal function during cadmium intoxication in the rat. Am J Physiol Renal Physiol 290:F127–F137

Jin YH, Clark AB, Slebos RJ et al (2003) Cadmium is a mutagen that acts by inhibiting mismatch repair. Nat Genet 34:326–329

Lee G, Schlichter L, Bendayan M, Bendayan R (2001) Functional expression of P-glycoprotein in rat brain microglia. J Pharmacol Exp Ther 299:204–212

Lee WK, Abouhamed M, Thévenod F (2006) Caspase-dependent and -independent pathways for cadmium-induced apoptosis in cultured kidney proximal tubule cells. Am J Physiol Renal Physiol 291:F823-F832

Lee WK, Bork U, Gholamrezaei F, Thévenod F (2005) Cd2+-induced cytochrome c release in apoptotic proximal tubule cells: role of mitochondrial permeability transition pore and Ca2+ uniporter. Am J Physiol Renal Physiol 288:F27-F39

Liu J, Habeebu SS, Liu Y, Klaassen CD (1998) Acute CdMT injection is not a good model to study chronic Cd nephropathy: comparison of chronic CdCl2 and CdMT exposure with acute CdMT injection in rats. Toxicol Appl Pharmacol 153:48–58

Matsuoka M, Call KM (1995) Cadmium-induced expression of immediate early genes in LLC-PK1 cells. Kidney Int 48:383–389

Miyoshi J, Takai Y (2005) Molecular perspective on tight-junction assembly and epithelial polarity. Adv Drug Deliv Rev 57:815–855

Mosmann T (1983) Rapid colorimetric assay for cellular growth and survival: application to proliferation and cytotoxicity assays. J Immunol Methods 65:55–63

Niewenhuis RJ, Dimitriu C, Prozialeck WC (1997) Ultrastructural characterization of the early changes in intercellular junctions in response to cadmium (Cd2+) exposure in LLC-PK1 cells. Toxicol Appl Pharmacol 142:1–12

Pesch B, Haerting J, Ranft U et al. (2000) Occupational risk factors for renal cell carcinoma: agent-specific results from a case-control study in Germany. MURC Study. Group Multicenter urothelial and renal cancer study. Int J Epidemiol 29:1014–1024

Polakis P (1999) The oncogenic activation of beta-catenin. Curr Opin Genet Dev 9:15–21

Prozialeck WC, Grunwald GB, Dey PM, Reuhl KR, Parrish AR (2002) Cadherins and NCAM as potential targets in metal toxicity. Toxicol Appl Pharmacol 182:255–265

Prozialeck WC, Lamar PC, Lynch SM (2003) Cadmium alters the localization of N-cadherin, E-cadherin, and beta-catenin in the proximal tubule epithelium. Toxicol Appl Pharmacol 189:180–195

Prozialeck WC, Niewenhuis RJ (1991a) Cadmium (Cd2+) disrupts Ca(2+)-dependent cell-cell junctions and alters the pattern of E-cadherin immunofluorescence in LLC-PK1 cells. Biochem Biophys Res Commun 181:1118–1124

Prozialeck WC, Niewenhuis RJ (1991b) Cadmium (Cd2+) disrupts intercellular junctions and actin filaments in LLC-PK1 cells. Toxicol Appl Pharmacol 107:81–97

Qu W, Fuquay R, Sakurai T, Waalkes MP (2006) Acquisition of apoptotic resistance in cadmium-induced malignant transformation: specific perturbation of JNK signal transduction pathway and associated metallothionein overexpression. Mol Carcinog 45:561–571

Rothen-Rutishauser B, Riesen FK, Braun A, Gunthert M, Wunderli-Allenspach H (2002) Dynamics of tight and adherens junctions under EGTA treatment. J Membr Biol 188:151–162

Sabolic I, Herak-Kramberger CM, Brown D (2001) Subchronic cadmium treatment affects the abundance and arrangement of cytoskeletal proteins in rat renal proximal tubule cells. Toxicology 165:205–216

Schinkel AH, Smit JJ, van Tellingen O et al. (1994) Disruption of the mouse mdr1a P-glycoprotein gene leads to a deficiency in the blood-brain barrier and to increased sensitivity to drugs. Cell 77:491–502

Singh BR, McLaughlin MJ (1999) Cadmium in soils and plants. In: McLaughlin MJ, Singh BR (eds), Developments in plant and soil sciences, vol. 85. Kluwer Academic Publishers, Dordrecht, pp 257–268

Takebayashi S, Jimi S, Segawa M, Kiyoshi Y (2000) Cadmium induces osteomalacia mediated by proximal tubular atrophy and disturbances of phosphate reabsorption A study of 11 autopsies. Pathol Res Pract 196:653–663

Thévenod F (2003) Nephrotoxicity and the proximal tubule. Insights from cadmium. Nephron Physiol 93:87–93

Thévenod F, Friedmann JM (1999) Cadmium-mediated oxidative stress in kidney proximal tubule cells induces degradation of Na+/K(+)-ATPase through proteasomal and endo-/lysosomal proteolytic pathways. FASEB J 13:1751–1761

Thévenod F, Friedmann JM, Katsen AD, Hauser IA (2000) Up-regulation of multidrug resistance P-glycoprotein via nuclear factor-kappaB activation protects kidney proximal tubule cells from cadmium- and reactive oxygen species-induced apoptosis. J Biol Chem 275:1887–1896

Verougstraete V, Lison D, Hotz P (2002) A systematic review of cytogenetic studies conducted in human populations exposed to cadmium compounds. Mutat Res 511:15–43

Vleminckx K, Kemler R (1999) Cadherins and tissue formation: integrating adhesion and signaling. Bioessays 21:211–220

Waisberg M, Joseph P, Hale B, Beyersmann D (2003) Molecular and cellular mechanisms of cadmium carcinogenesis. Toxicology 192:95–117

Wegener J, Keese CR, Giaever I (2000) Electric cell-substrate impedance sensing (ECIS) as a noninvasive means to monitor the kinetics of cell spreading to artificial surfaces. Exp Cell Res 259:158–166

Wolff NA, Abouhamed M, Verroust PJ, Thevenod F (2006) Megalin-dependent internalization of cadmium-metallothionein and cytotoxicity in cultured renal proximal tubule cells. J Pharmacol Exp Ther 318:782–791

Woost PG, Orosz DE, Jin W et al. (1996) Immortalization and characterization of proximal tubule cells derived from kidneys of spontaneously hypertensive and normotensive rats. Kidney Int 50: 125–134

Yamada T, Mori Y, Hayashi R et al. (2003) Suppression of intestinal polyposis in Mdr1-deficient ApcMin/+ mice. Cancer Res 63:895–901

Zalups RK, Koropatnick J (2000) Molecular biology and toxicology of metals. Taylor and Francis, London, U.K. and New York, NY

Zimmerhackl LB, Momm F, Wiegele G, Brandis M (1998) Cadmium is more toxic to LLC-PK1 cells than to MDCK cells acting on the cadherin-catenin complex. Am J Physiol 275:F143–F153